

Northumbria Research Link

Citation: Dodd, Linzi, Geraldi, Nicasio, Xu, Ben, McHale, Glen, Wells, Gary, Stuart-Cole, Simone, Martin, James, Newton, Michael and Wood, David (2016) Low friction droplet transportation on a substrate with a selective Leidenfrost effect. *ACS Applied Materials & Interfaces*, 8 (34). pp. 22658-22663. ISSN 1944-8244

Published by: American Chemical Society

URL: <http://pubs.acs.org/doi/abs/10.1021/acsami.6b06738>
<<http://pubs.acs.org/doi/abs/10.1021/acsami.6b06738>>

This version was downloaded from Northumbria Research Link:
<http://nrl.northumbria.ac.uk/27437/>

Northumbria University has developed Northumbria Research Link (NRL) to enable users to access the University's research output. Copyright © and moral rights for items on NRL are retained by the individual author(s) and/or other copyright owners. Single copies of full items can be reproduced, displayed or performed, and given to third parties in any format or medium for personal research or study, educational, or not-for-profit purposes without prior permission or charge, provided the authors, title and full bibliographic details are given, as well as a hyperlink and/or URL to the original metadata page. The content must not be changed in any way. Full items must not be sold commercially in any format or medium without formal permission of the copyright holder. The full policy is available online: <http://nrl.northumbria.ac.uk/policies.html>

This document may differ from the final, published version of the research and has been made available online in accordance with publisher policies. To read and/or cite from the published version of the research, please visit the publisher's website (a subscription may be required.)

www.northumbria.ac.uk/nrl



Low friction droplet transportation on a substrate with a selective Leidenfrost effect

By Linzi E. Dodd¹*, Nicasio R. Geraldi², Ben B. Xu², Glen McHale², Gary G. Wells², Simone Stuart-Cole³, James Martin³, Michael I. Newton⁴, and David Wood¹

¹ Dr Linzi E. Dodd, Prof. David Wood
Microsystems Technology Group,
School of Engineering & Computing Sciences,
Durham University,
Durham, DH1 3LE, UK

² Dr Nicasio R. Geraldi, Dr Gary G. Wells, Prof. Glen McHale, Dr Ben B. Xu,
Smart Materials and Surfaces Lab,
Faculty of Engineering and Environment,
Northumbria University,
Newcastle upon Tyne, NE1 8ST, UK

³ Dr Simone Stuart-Cole, Dr James Martin
Reece Innovation,
Armstrong Works, Scotswood Road,
Newcastle upon Tyne, NE15 6UX, UK

⁴ Dr Michael I. Newton
School of Science and Technology,
Nottingham Trent University,
Nottingham, NG11 8NS, UK

* To whom correspondence should be addressed. E-mail: l.e.dodd@durham.ac.uk

KEYWORDS: Droplet transportation, Leidenfrost effect, Selective heating, Microengineering, MEMS

ABSTRACT

An energy saving Leidenfrost levitation method is introduced to transport micro-droplets with virtually frictionless contact between the liquid and solid substrate. By micro-engineering the heating units, selective areas of the whole substrate can be electro-thermally activated. A droplet can be levitated as a result of the Leidenfrost effect, and further transported when the substrate is tilted slightly. The selective electro-heating produces a uniform temperature distribution on the heating units within 1 s, in response to a triggering voltage. Alongside these experimental observations, finite element simulations are conducted to understand the role of the substrate thermal conductivity on the temperature profile of the selectively heated substrate. We also generate phase diagrams to verify the Leidenfrost regime for different substrate materials. Finally, we demonstrate the possibility of controlling low friction high speed droplet transportation (~ 65 mm/s) when the substrate is tilted ($\sim 7^\circ$) by structurally designing the substrate. This work establishes the basis for an entirely new approach to droplet microfluidics.

INTRODUCTION

Transporting droplets in a controllable and energy efficient manner could have a significant impact on several engineering applications, such as low drag liquid transportation^{1,2}, water collection^{3,4}, and advanced microfluidic devices⁵. Based on a theoretical understanding of the wetting of surfaces, common approaches usually focus on creating a surface with designed physical/chemical features, e.g. hierarchical micro/nanostructured surfaces^{6,7}, chemical gradients^{8,9}, or slippery surfaces created by infusing low surface tension lubricant into microstructures that yield directional motion of water droplets when tilted at a low angle¹⁰⁻¹². Notably, some interesting attempts have demonstrated liquid transportation efficiency using such

1
2
3 techniques: for example, Chaudhury and Whitesides achieved an average velocity of 1–2 mm/s
4
5 for droplet transportation on a silicon wafer possessing a gradient in wettability¹³, Ghosh *et al.*
6
7 employed extreme wettability patterns to achieve a flow rate of up to 300 mm/s¹⁴, and Lv *et al.*
8
9 achieved a maximum speed of 420 mm/s for droplet transportation in a microfluidic system¹⁵.
10
11 Approaches taken to date have been based on the liquid-solid contact, where the droplet motion
12
13 will more or less be affected by the friction or dragging effect induced by local surface
14
15 roughness, dimensional confinement, as well as the non-uniformity of the surface wettability.
16
17
18
19

20
21 The Leidenfrost phenomenon (Figure 1a), first discovered in 1756¹⁶, describes a meta-stable
22
23 state of a droplet on a substrate heated significantly above the boiling point of the liquid. In this
24
25 state, the droplet is levitated by an instantaneously generated vapor layer (~ 100-200 μm) caused
26
27 by the initial contact of the droplet with the substrate¹⁷⁻²¹. The levitation yields a virtually
28
29 frictionless contact between the droplet and substrate²¹⁻²³, therefore playing a key role in drag
30
31 reduction for the liquid flow^{24,25}. Moreover, the vapor layer acts as a thermal insulator preventing
32
33 rapid droplet evaporation despite the high temperature of the substrate. Recent developments
34
35 show some attempts to control the droplet motion based on the Leidenfrost effect levitation by
36
37 employing ratcheted and other patterned substrates^{21,26-29}, magnetic fields³⁰, electric fields³¹ and
38
39 acoustic radiation pressure³². However, the actuation of the Leidenfrost effect for a droplet has
40
41 thus far involved heating the entire substrate, which limits downstream applications due to the
42
43 extreme substrate temperature condition. Despite recent work to reduce the transition
44
45 temperature^{24,28}, the high energy consumption remains due to heating the substrate globally,
46
47 rather than the localized area which supports the droplet.
48
49
50
51
52
53
54

55 In this study, we trigger Leidenfrost levitation of a droplet by the application of a voltage to
56
57 micron-scaled serpentine shaped heating arrays, which cover the substrate in a selective manner.
58
59
60

1
2
3 In addition to initializing the levitation of droplets of three different liquids via selective heating
4 of substrate areas, we also show that the droplet transportation can be actuated and controlled by
5 designing heating array patterns, along with tilting of the substrate (5–10 °). The proposed
6 strategy of selective heating could significantly reduce the energy input needed to actuate the
7 Leidenfrost effect, and also offer a control mechanism for droplet motion by locally controlling
8 the designed heating array. By combining our approach with surface relief patterns, precise
9 directional control and self-propulsion can be achieved without the need to tilt a surface³³. It also
10 enables the possible integration of levitation of droplets into micro-systems as a new type of on-
11 chip platform.
12
13
14
15
16
17
18
19
20
21
22
23
24

25 EXPERIMENTAL

26
27
28
29 **Micro-fabrication:** Thin film resistors were fabricated on different substrates, i.e. borosilicate
30 glass and silicon (with oxidation layer) wafers. After cleaning the substrate, a thin film metal
31 layer (Cr/Au = ~10 nm/~100 nm in thicknesses) was coated on the substrate via electron beam
32 evaporation. The resistor patterns were photolithographically transferred into the metal layer by
33 spinning Megaposit SPR-350 photoresist, which was exposed to UV light in an EVG mask
34 aligner and then developed in Microposit MF-319 developer for 90 s. The excess metal out of the
35 photoresist's protection was removed using selective gold (4:1:8 KI:I₂:H₂O) and chromium
36 (7:34:1 Ce(NH₄)₂(NO₃)₆:HNO₃:H₂O) wet etches, leaving the required resistor patterns with
37 varying distance between consecutive lines.
38
39
40
41
42
43
44
45
46
47
48
49
50

51 **Leidenfrost Levitation Activation and Measurements:** Each wafer was selectively covered by
52 4 two dimensional arrays of devices, and electrical contact pads for each array were designed to
53 enable independent control of the heating arrays. A customized rig was assembled with a
54
55
56
57
58
59
60

1
2
3 stainless steel stage on an $x y z \theta$ manipulator, to assist the characterization. In order to maintain
4
5 a uniform temperature within the stage, an mbed-controlled Peltier cooler with cooling pipes and
6
7 fan was mounted on the underside of the stage to stabilize the ambient condition. Spring loaded
8
9 electrical contacts were then used to pass a current through each array in turn. To verify the
10
11 effectiveness of the Leidenfrost Levitation, we tested three different liquids, isopropanol (surface
12
13 tension ~ 20 mN/m), acetone (surface tension ~ 28 mN/m), and deionized water (surface tension
14
15 ~ 72 mN/m). All liquids produced similar results, once heated beyond their respective
16
17 Leidenfrost transition temperatures. In this paper, we present the summarized results for IPA as a
18
19 typical case for the lowest surface tension liquid, which is the most difficult liquid when
20
21 attempting to use materials techniques to create a super-liquid-repellent state. A 1000x USB
22
23 optical microscope was used to observe the arrays, and a FLIR A40 thermal camera was used to
24
25 observe the temperature profile of the substrate. Different powers were applied to each heated
26
27 array in turn, and the array was left for 1 minute for the temperature to equalize.
28
29
30
31
32
33

34
35 **Simulation:** A ‘unit cell’ device was also modelled in COMSOL Multiphysics software, which
36
37 also included the substrate, stage and effects of the Peltier cooling as a boundary condition. The
38
39 COMSOL model involves parameterized substrate gaps between consecutive unit cells, and so
40
41 all heating ratios can be simulated automatically. The substrate either side of the unit cell is
42
43 related to the heated ratio, with the end of the substrate being the halfway point between two unit
44
45 cells, which would be the coldest point in the array and therefore the region most likely to cause
46
47 a collapse in the Leidenfrost vapor layer. All of the solid vertical boundaries in this model have a
48
49 symmetry condition, whereas the air has an outflow condition. Finally, the bottom of the
50
51 stainless steel domain has a fixed temperature boundary condition (21 °C), to simulate the Peltier
52
53 cooler placed underneath the stainless steel stage.
54
55
56
57
58
59
60

RESULTS AND DISCUSSION

In our experiments, the concept of selective electro-thermally actuating Leidenfrost levitation is achieved by engineering millimeter-scale heating units on the substrate. The heating units covering the substrate are intended to create a uniform distribution of the thermal energy to trigger the Leidenfrost effect (Figure 1b), but in a selective manner only where this is needed to levitate a droplet. Different substrates (borosilicate glass and silicon) were used to determine the effect of the substrate thermal conductivity on the power needed for the Leidenfrost effect to occur. Since the thermal conductivities for borosilicate and silicon are 1.14 W/mK and 1480 W/mK respectively, these choices provide over three orders of magnitude difference with this parameter³². The silicon substrates were electrically insulated via a 100 nm thick silicon dioxide layer, grown by furnace oxidation, between the substrate and the heating array layer. In preliminary experiments we confirmed that the Leidenfrost effect could be achieved with droplets of isopropanol (IPA), acetone, and deionized water. Once the Leidenfrost effect was triggered, virtually frictionless liquid transportation was expected on a pre-tilted substrate.

We first consider a substrate patterned with relatively large heating units arranged in 2.5 mm width bands. After tilting the substrate by $\sim 7^\circ$, the levitated isopropanol (IPA) droplet ($\sim 40 \mu\text{L}$) is transported across a distance of 17.5 mm on the substrate in 0.27 seconds, i.e. $\sim 65 \text{ mm/s}$, indicating very low friction (Figure 1c). The Leidenfrost effect usually represents a meta-stable state of droplet when it comes into contact with a surface that is significantly hotter than the liquid's boiling point. Typically, a vapor layer will be initialized to support, and so yield a longer lifetime, of the droplet, and enable a virtually frictionless contact between the drop and the substrate. The droplet transportation supported by an electro-thermally actuated Leidenfrost effect is demonstrated for the first time in this report.

1
2
3 The actuation of Leidenfrost effect was further investigated by designing and patterning micron-
4 scaled heating arrays onto substrates. To quantitatively evaluate the electro-heating actuation of
5 the Leidenfrost effect, we designed the serpentine-shaped repeating ‘unit cell’ (Figure 2a) to
6 further reduce the surface coverage to 62.5% of the overall area of the heated region. A defined
7 geometrical parameter, the heating ratio, which is a 1 dimensional ratio between heated and
8 unheated regions, where $p = 40 \mu\text{m}$ and represents the width of the heated region, and the ratio is
9 $p:(p + d)$, where d is the distance between consecutive unit cells, seen in the inset of Figure 2b.
10
11 The total area heated for a given ratio can be calculated by multiplying the heated ratio by the
12 serpentine unit cell coverage. For example, for a 0.2 heated ratio, the total heated percentage
13 would be 20% multiplied by 62.5%, which is 12.5% of the area being heated. A typical plot of
14 evaporation time versus input power on a heated 2D array of unit cells, shown in Figure 2b, is
15 similar to previous results using more conventional methods (e.g. hotplate heated devices)
16 (Figure S-1). In Figure 2b, the Leidenfrost transition (dotted line) is monitored by recording the
17 evaporation time of a droplet, t_{eva} , as a function of the power input for a 0.5 heated ratio array.
18
19 The dotted line of 21.8 W is the typical power value needed to boil the IPA droplet (for these
20 experiments, a 20 μL volume was used) for this heated ratio, whereby the IPA touches the hot
21 surface and evaporates due to the high temperature of the surface below it. Above this power, the
22 transition regime denotes a region where the substrate is hot enough to begin creating a localized
23 vapor underneath the droplet, but the temperature is not yet high enough to do this in a stable
24 way, and the vapor layer is not thick enough to maintain a levitating droplet. In the stable
25 Leidenfrost regime (right of the dotted line), the vapor can maintain a stable levitated state for
26 the droplet. The determination of transition regime under selectively heated electrical actuation
27 reveals a strong similarity to that from global heating of the substrate.
28
29
30
31
32
33
34
35
36
37
38
39
40
41
42
43
44
45
46
47
48
49
50
51
52
53
54
55
56
57
58
59
60

1
2
3 In contrast to heating a substrate globally, selective heating to create discontinuously heated
4 fields across the in-plane area of the substrate should reduce the energy input. To understand
5 how the thermal energy distributes across the substrate, we performed surface thermal analysis
6 using COMSOL Multiphysics. The qualitative analysis (Figure 3a) first considers a serpentine
7 ‘unit cell’ resistor (0.2 heated ratio) on a borosilicate glass substrate with a voltage applied to
8 show the temperature profile of the single unit cell above the Leidenfrost transition temperature.
9 The heat created as a result is then dissipated through the substrate, the stage underneath and also
10 the air above the resistor. As can be seen in Figure 3a, the temperature difference across a
11 distance of 100 μm , from the center of the heat to half way between two unit cells (or a heated
12 ratio of 0.2) is as high as 20 $^{\circ}\text{C}$ for the borosilicate glass substrate.
13
14
15
16
17
18
19
20
21
22
23
24
25
26
27

28 As a result of this temperature difference, it would be expected that the resistors with a lower
29 heated ratio (or a larger gap between them) would have to be heated to a higher temperature than
30 required, in order to get the coolest part of the array to still be hot enough for the Leidenfrost
31 effect to occur. To prove this, we further simulate the unit cells, with three adjacent serpentine
32 units shown here on the same substrate (Figure 3b) with a voltage applied on each unit cell
33 (heated ratio = 0.5), and demonstrate a more uniform distribution of the temperature (the
34 difference of temperature is less than 5 $^{\circ}\text{C}$). In this case, the voltage required is lower than for the
35 unit cell shown in Figure 3a. We note that the current flow through the serpentine-shaped unit
36 cell is non-uniform as a result of the structure’s geometry, as can be seen in Figure S-2, and the
37 subsequent thermal stress localization could potentially lead to mechanical failure. However, no
38 failures occurred in our experiment and this may have been because the localized strain energy
39 was likely absorbed by the in-plane structural expansion and the chromium adhesion layer.
40
41
42
43
44
45
46
47
48
49
50
51
52
53
54
55
56
57
58
59
60

1
2
3 Using the selectively heated substrate with repeated unit cell (heated ratio = 0.5), we next plot
4 the phase diagrams to describe the meta-stable state of the heated IPA droplet on a glass
5 substrate (Figure 3c) and a silicon substrate (Figure 3d). Experimental data are compared with
6 the COMSOL simulation results. The Leidenfrost state is shown in the diagram and the
7 anticipated trend of reducing power being needed to initiate the Leidenfrost effect when
8 increasing the heating ratio is observed. There is good agreement between the experimental and
9 simulated results, where the model assumes a Leidenfrost temperature of 220 °C, which is a
10 reasonable value for IPA which has a boiling point of 82.4 °C³⁴.
11
12

13
14
15
16
17
18
19
20
21
22
23 As the selectivity of the Leidenfrost effect is via voltage actuated heating units on the substrate,
24 the thermal conductivity of the latter will have a direct influence on the results. Two substrate
25 materials with a large difference on thermal conductivity were employed to verify this impact,
26 i.e. borosilicate glass (1.14 W/mK) and silicon (1480 W/mK) at 300 K³². As can be seen in
27 Figure 3d, the results for a silicon substrate still follow the decreasing trend with increasing
28 heated ratio. However, a greater power per line is required than for the borosilicate substrates to
29 achieve the Leidenfrost effect, because the heat is dissipated through the substrate more readily,
30 rather than remaining in the vicinity of the serpentine-shaped unit cells to form the uniform in-
31 plane temperature profile. Therefore, borosilicate is a more preferable substrate material for this
32 experiment, as it could create a uniform temperature profile more effectively on the surface of
33 the substrate, owing to its low thermal conductivity.
34
35
36
37
38
39
40
41
42
43
44
45
46
47
48
49

50 Finally, we demonstrate the possibility of controlling droplet transportation by taking advantage
51 of using a selectively heated substrate (Figure S-3). A substrate with four separate blocks of 0.5
52 ratio heating arrays, each of which could be individually switched in sequence was created, as
53 seen in Figure 4a and 4b. The first, second and fourth arrays were switched on for 0.1 s in turn,
54
55
56
57
58
59
60

1
2
3 with a 0.1 s time gap between each one being switched on. Therefore, the substrate was
4
5 selectively heated in the micro-scale (due to the heated ratio), the macro scale (the four arrays
6
7 being heated individually) and in time (the arrays being sequenced individually). Each array was
8
9 activated for an eighth of a cycle. The third array was left disconnected. A schematic of the
10
11 controlled droplet transportation shows the droplet to the target zone (un-activated region)
12
13 possessing the disconnected heating array in a short time. Experimental images (Figure 4c and
14
15 4d) indicate rapid droplet movements from both directions to region #3, at a comparable speed to
16
17 that witnessed in Figure 1c, thus implying rapid, virtually frictionless transport. This concept also
18
19 enables a new strategy of targeted delivery of a droplet by configuring the substrate to form, on
20
21 demand, localized frictionless levitation layers, which could be of considerable interest to
22
23 scientists and researchers in micro-fluidic systems, chemical engineering, biological engineering
24
25 and other related areas.
26
27
28
29
30

31 32 CONCLUSION

33
34
35
36 In conclusion, we have demonstrated the electro-heating actuation of the Leidenfrost effect for
37
38 three different liquids by applying voltages to heating units which selectively cover a substrate.
39
40 This approach provides rapidly switchable and highly targeted transportation of droplet,
41
42 according to the design of the geometry and layout of the heating array on the substrate. By
43
44 selectively heating a sample to produce the Leidenfrost effect in a small area where needed,
45
46 rather than using a hot plate to heat the entire surface, the same effect can be achieved but with a
47
48 much lower energy requirement. It also provides the potential for easy integration to be part of
49
50 an on-chip device with an electrical triggering mechanism. Moreover, further energy efficiency
51
52 could be achieved by using a feedback control system to drive and control the direction of
53
54
55
56
57
58
59
60

1
2
3 motion of droplets with actuation only of those heating units in the instantaneous locality of the
4
5 levitated droplet.
6
7

8 9 ACKNOWLEDGEMENTS

10
11
12 The work was supported by the Engineering and Physical Sciences Research Council (EPSRC)
13 through grants EP/L026899/1, EP/L026619/1 and EP/L026341/1. The authors also acknowledge
14
15 funding from the EU-COST MP1106 network.
16
17
18

19 20 SUPPORTING INFORMATION

- 21
22
23
- 24 • **Figure S-1.** The Leidenfrost transition graph for a sample on a hotplate
 - 25
26
27 • **Figure S-2.** COMSOL image of flow of current through serpentine resistor on a
28 borosilicate substrate.
 - 29
30
31
32
33 • **Movie S-3.** Video showing targeted transportation of a droplet upon selective heated
34 substrate. We show the instant droplet transportations from both directions to expected
35 destination when we applied a voltage of 60 V to the settings in Figure 4a and 4b. The
36 droplet travels within 1 second and stopped at the non-activated area (#3).
37
38
39
40
41
42
43
44
45
46
47
48
49
50
51
52
53
54
55
56
57
58
59
60

REFERENCES:

- (1) Bhushan, B.; Jung, Y.C. Natural and Biomimetic Artificial Surfaces for Superhydrophobicity, Self-Cleaning, Low Adhesion, and Drag Reduction *Prog. Mater. Sci.* **2011**, 56, 1-108.
- (2) Liu, K.; Jiang, L. Bio-Inspired Self-Cleaning Surfaces *Ann. Rev. Mater. Res.* **2012**, 42, 231-263.
- (3) Zhao, B.; Moore, J.S.; Beebe, D.J. Surface-Directed Liquid Flow Inside Microchannels *Science* **2001**, 291, 1023-1026.
- (4) Yao, X.; Song, Y.; Jiang, L. Applications of Bio-Inspired Special Wettable Surfaces *Adv. Mater.* **2011**, 23, 719-734.
- (5) Ionov, L.; Houbenov, N.; Sidorenko, A.; Stamm, M.; Minko, S. Smart Microfluidic Channels *Adv. Funct. Mater.* **2006**, 16, 1153-1160.
- (6) Feng, L.; Li, S.; Li, Y.; Li, H.; Zhang, L.; Zhai, J.; Song, Y.; Liu, B.; Jiang, L.; Zhu, D. Super-Hydrophobic Surfaces: From Natural to Artificial *Adv. Mater.* **2002**, 14, 1857-1860.
- (7) Zheng, Y.; Gao, X.; Jiang, L. Directional Adhesion of Superhydrophobic Butterfly Wings *Soft Matter* **2007**, 3, 178-182.
- (8) Zhang, J.; Han, Y. Shape-Gradient Composite Surfaces: Water Droplets Move Uphill *Langmuir* **2007**, 23, 6136-6141.

1
2
3 (9) Bliznyuk, O.; Seddon, J.R.T.; Veligura, V.; Kooij, E.S.; Zandvliet, H. J. W.; Poelsema, B.
4 Directional Liquid Spreading over Chemically Defined Radial Wettability Gradients *ACS Appl.*
5 *Mater. Interfaces* **2012**, 4, 4141-4148.
6
7

8
9
10
11 (10) Kim, P.; Kreder, M.J.; Alvarenga, J.; Aizenberg, J. Hierarchical or Not? Effect of the
12 Length Scale and Hierarchy of the Surface Roughness on Omniphobicity of Lubricant-Infused
13 Substrates *Nano Lett.* **2013**, 13, 1793-1799.
14
15

16
17
18
19 (11) Smith, J.D.; Dhiman, R.; Anand, S.; Reza-Garduno, E.; Cohen, R.E.; McKinley, R.H.;
20 Varanasi, K.K. Droplet Mobility on Lubricant-Impregnated Surfaces *Soft Matter* **2013**, 9, 1772-
21 1780.
22
23
24

25
26
27 (12) Yao, X.; Hu, Y.; Grinthal, A.; Wong, T.S.; Mahadevan, L.; Aizenberg, J. Adaptive Fluid-
28 Infused Porous Films with Tunable Transparency and Wettability *Nat. Mater.* **2013**, 12, 529-534.
29
30

31
32 (13) Chaudhury, M.K.; Whitesides, G.M. How To Make Water Run Uphill *Science* **1992**, 256,
33 1539-1541.
34
35
36

37
38 (14) Ghosh, A.; Ganguly, R.; Schutzius, T.M.; Megaridis, C.M. Wettability Patterning for High-
39 Rate, Pumpless Fluid Transport on Open, Non-Planar Microfluidic Platforms *Lab Chip* **2014**, 14,
40 1538-1550.
41
42
43

44
45 (15) Lv, C.; Chen, C.; Chuang, Y.C.; Tseng, F.G.; Yin, Y.; Grey, F.; Zheng, Q. Substrate
46 Curvature Gradient Drives Rapid Droplet Motion *Phys. Rev. Lett.* **2014**, 113, 026101.
47
48
49

50
51 (16) Leidenfrost, J.G. On Fixation of Water in Diverse Fire *Int. J. Heat Mass. Transfer* **1966**, 9,
52 1153 (translated by C. Wares).
53
54
55
56
57
58
59
60

- 1
2
3 (17) Biance, A.L.; Clanet, C.; Quéré, D. Leidenfrost Drops *Phys. Fluids*. **2003**, 15, 1632.
4
5
6
7 (18) Dupeux, G.; Le Merrer, M.; Clanet, C.; Quéré, D. Trapping Leidenfrost Drops with
8
9 Crenelations *Phys. Rev. Lett.* **2011**, 107, 114503.
10
11
12 (19) Dupeux, G.; Le Merrer, M.; Lagubeau, G.; Clanet, C.; Hardt, S.; Quéré, D. Viscous
13
14 Mechanism for Leidenfrost Propulsion on a Ratchet *EPL* **2011**, 96, 58001.
15
16
17
18 (20) Celestini, F.; Frisch, T.; Pomeau, Y. Take Off of Small Leidenfrost Droplets *Phys. Rev. Lett.*
19 **2012** 109, 034501.
20
21 (21) Dupeux, G.; Bourriane, P.; Magdelaine, Q.; Clanet, C.; Quéré, D. Propulsion on a
22
23 Superhydrophobic Ratchet *Sci. Rep.* **2014**, 4, 5280.
24
25
26
27 (22) Quéré, D. Leidenfrost Dynamics *Annu. Rev. Fluid. Mech.* **2013**, 45, 197-215.
28
29
30 (23) Wells, G.G.; Ledesma-Aguilar, R.; McHale, G.; Sefiane, K. A Sublimation Heat Engine
31
32 *Nat. Comm.* **2015**, 6, 6390.
33
34
35
36 (24) Vakarelski, I.U.; Patankar, N.A.; Marston, J.O.; Chan, D.Y.C.; Thoroddsen, S.T.
37
38 Stabilization of Leidenfrost Vapour Layer by Textured Superhydrophobic Surfaces *Nature* **2012**,
39
40 489, 274-277.
41
42
43
44 (25) Vakarelski, I.U.; Marston, J.O.; Chan, D.Y.C.; Thoroddsen, S.T. Drag Reduction by
45
46 Leidenfrost Vapor Layers *Phys. Rev. Lett.* **2011**, 106, 214501.
47
48
49
50 (26) Lagubeau, G.; Le Merrer, M.; Clanet, C.; Quéré, D. Leidenfrost on a Ratchet *Nat. Phys.*
51
52 **2011**, 7, 395-398.
53
54
55
56
57
58
59
60

- 1
2
3 (27) Ok, J. T.; Lopezona, E.; Nikitopoulos, D. E.; Wong, H.; Park, S. Propulsion of Droplets on
4 Micro- and Sub-Micron Ratchet Surfaces in the Leidenfrost Temperature Regime *Microfluid.*
5 *Nanofluid.* **2010**, 10, 1045-1054.
6
7
8
9
10
11 (28) Feng, R.; Zhao, W.; Wu, X.; Xue, Q. Ratchet Composite Thin Film for Low-Temperature
12 Self-Propelled Leidenfrost Droplet *J. Colloid Interface Sci.* **2012**, 367, 450-454.
13
14
15
16
17 (29) Geraldi, N.R.; McHale, G.; Xu, B.B.; Wells, G.G.; Dodd, L.E.; Wood, D.; Newton, M.I.
18 Leidenfrost Transition Temperature for Stainless Steel Meshes *Mater. Lett.* **2016**, 176, 205–208.
19
20
21
22 (30) Piroird, K.; Clanet, C.; Quéré, D. Magnetic Control of Leidenfrost Drops *Phys. Rev. E: Sta.,*
23 *Nonlinear, and Soft Matter Phys.* 2012, 85, 056311.
24
25
26
27
28 (31) Wang, Y.; Bhushan, B. Liquid Microdroplet Sliding on Hydrophobic Surfaces in the
29 Presence of an Electric Field *Langmuir* **2010**, 26, 4013-4017.
30
31
32
33
34 (32) Ng, B.T.; Hung, Y.M.; Tan, M.K.; Acoustically-Controlled Leidenfrost Droplets *J. Colloid*
35 *Interface Sci* **2016**, 465, 26-32.
36
37
38
39
40 (33) Linke, H.; Alemán, B.J.; Melling, L.D.; Taormina, M.J.; Francis, M.J.; Dow-Hygelund,
41 C.C.; Narayanan, V.; Taylor, R.P.; Stout, A. Self-Propelled Leidenfrost Droplets *Phys. Rev. Lett.*
42 **2006**, 96, 154502.
43
44
45
46
47
48 (34) Lide, D.R. *CRC Handbook of Chemistry and Physics 74th edition*, CRC Press, **1993**.
49
50
51
52
53
54
55
56
57
58
59
60

FIGURES

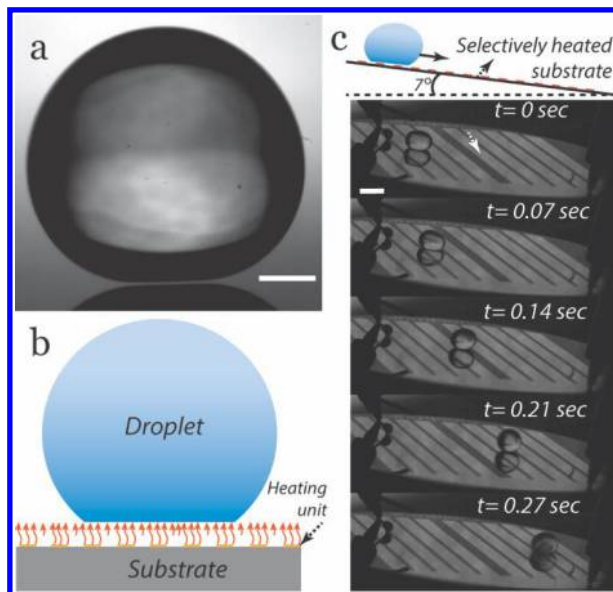


Figure 1. Initializing the Leidenfrost effect by creating localized Joule heating areas with selective coverage of heating units on a substrate. (a) A side view image of a traditional Leidenfrost levitated water droplet on a heated silicon wafer surface ($\sim 300\text{ }^{\circ}\text{C}$); the scale bar is $500\text{ }\mu\text{m}$. (b) Schematic illustration of Leidenfrost levitation on a substrate selectively covered by metal heating units. (c) The concept is examined through virtually frictionless transportation of an IPA droplet ($\sim 40\text{ }\mu\text{L}$), supported by the levitation vapor layer. The substrate is selectively covered by heating units in bands of width 2.5 mm (indicated by white the arrow) indicating droplet transportation speeds of $\sim 65\text{ mm s}^{-1}$; the substrate is tilted by 7° and the scale bar is 2 mm .

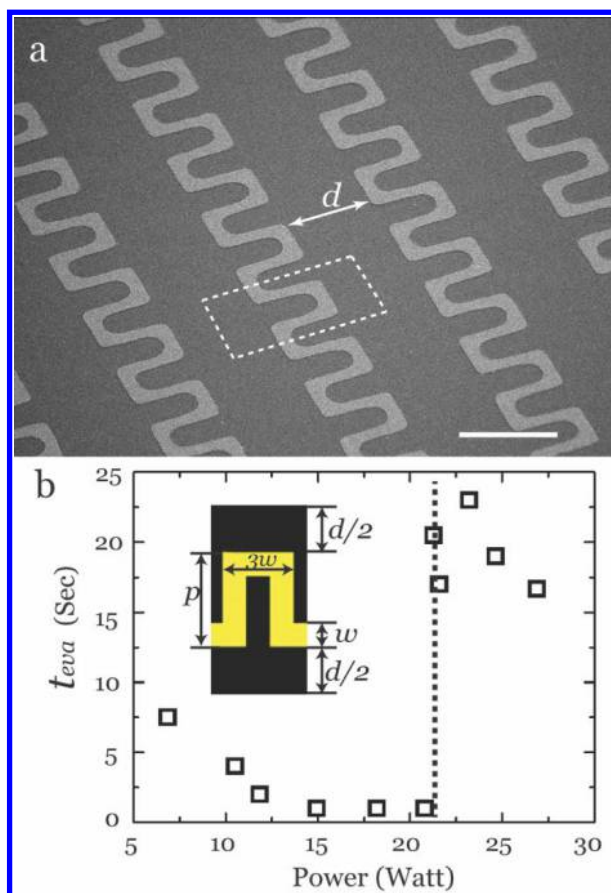


Figure 2. Micro-pattern of gold heating units and detection of the critical Leidenfrost transition.

(a) SEM image of micro-patterned chromium/gold heating array using serpentine patterns defined by an electrode width $w = 10 \mu\text{m}$, gap distance d , and electrode structure width $p = 40 \mu\text{m}$. (b) The Leidenfrost transition (dotted line) is monitored by recording the evaporation time of a droplet, t_{eva} , as a function of the power input. The inset shows the unit cell design within a serpentine electrode for selective heating of the substrate (the heated area is the lighter area), where the overall unit area is shown by the dashed box in (a).

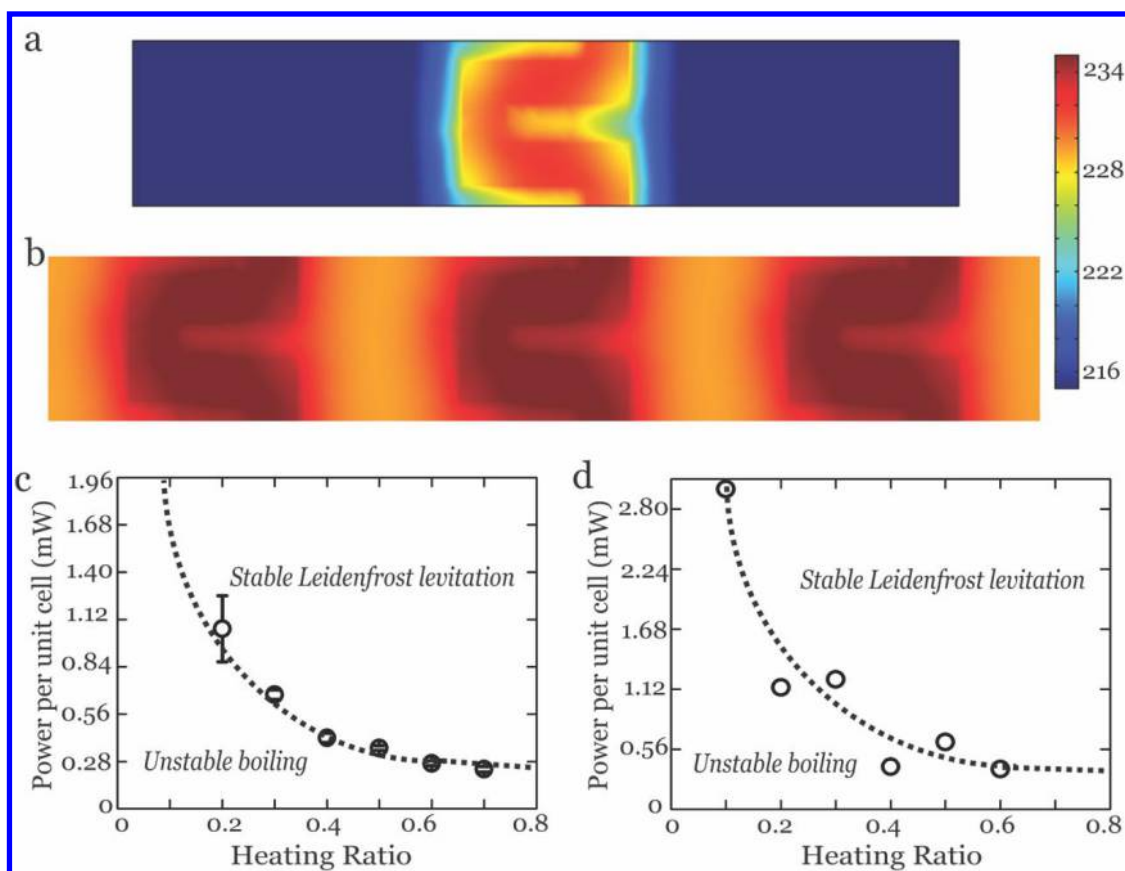


Figure 3. Selective Leidenfrost mechanism and phase diagrams. (a) Temperature profile of surface for the electro-heating of single unit cell with a 0.2 heated ratio. The COMSOL simulation in (b) reveals a uniform distribution of the temperature (in degrees Celsius) across the unit cells within three adjacent serpentine units (a heated ratio of 0.5). The simulation is based on 363 serpentine unit cells in series, which are referred to as a line, and a number of these lines are connected in parallel to form a complete heating array. The applied voltage is then varied to provide an equivalent power per cell required for the Leidenfrost effect to occur. The selective Leidenfrost effect using this pattern is described by phase diagrams on (c) a glass substrate and (d) a silicon substrate. The dotted lines represent the simulation results and the symbols represent the experimental results, respectively.

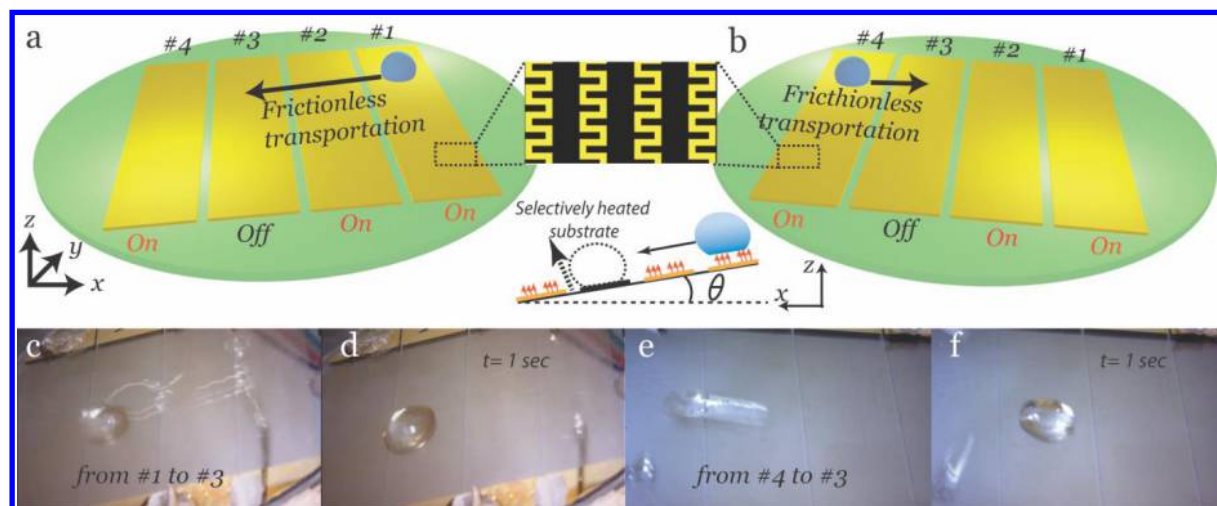


Figure 4. Demonstration of droplet transportation using programmable activation of localized heating units. (a-b) Schematic illustrations of experimental arrangements with example designs which selectively cover a substrate with four micro-patterned heating arrays (numbered #1 to #4 from right to left); each complete unit consists of serpentine-patterned unit cells as illustrated by Figure 2a. The third unit is non-activated to give an ‘off’ state while the others are activated into an ‘on state’. The whole wafer is tilted at a small angle of 10° in (a) and -10° in (b), as shown in the inset side view schematic. The droplet travels downslope across regions #1 and #2 with almost no friction due to the Leidenfrost effect, but then stops when it reaches the non-activated region #3; droplet transport is also stopped on the non-activated region when the substrate tilt is reversed (b). (c) Momentary snap shot of the droplet transportation shows the droplet advances from region #1 to region #3 with the setting in (a), and finally stopped at the non-activated region #3 (d). (e-f) Experimental images for droplet transport records the rapid virtually frictionless droplet transport from region #4 to region #3 with the setting (b).

GRAPHIC FOR MANUSCRIPT

